Scientia Iranica B (2012) 19 (6), 1564–1571

Sharif University of Technology

Scientia Iranica

Transactions B: Mechanical Engineering

www.sciencedirect.com

Research note

Effects of material properties on mechanical performance of Nitinol stent designed for femoral artery: Finite element analysis

F. Nematzadeh [a], **S.K. Sadrnezhaad** [b,*]

[a] *Materials and Energy Research Center (MERC), Tehran, P.O. Box 14155-4777, Iran*

[b] *Department of Materials Science and Engineering, Sharif University of Technology, Tehran, P.O. Box 11155-9466, Iran*

Received 27 July 2012; revised 14 September 2012; accepted 26 September 2012

KEYWORDS

Femoral artery;
Nitinol stent;
Material properties;
Mechanical performance;
Finite element analysis.

Abstract The Finite element method was used for evaluation of the effects of material properties on the mechanical performance of the new geometry designed for the *Z*-shaped open-cell femoral artery self-expanding stent, made of Nitinol wire, by application of crushing force. The behavior of the stents, having two sets of properties, was compared. The stents with higher A_f temperature show better clinical behavior due to lower chronic outward force, higher radial resistive strength and more suitable superelastic behavior. Model calculations show that a large change of A_f temperature could exert a substantial effect on the practical performance of the stent.

1. Introduction

Stenosis of the Superficial Femoral Artery (SFA) is one of the well-known diseases related to the vascular system [1]. Treating this disease is complicated, owing to the involvement of variable lengths of arteries and the divergent forces needed for flexion, torsion and compression. Aging and atherosclerosis have resulted in many geometric and material changes in SFA [2].

Percutaneous Transluminal Angioplasty (PTA) has been used as an acceptable treatment for femoral occlusive disease. Long-term results have, however, been considered suboptimal [1,2].

Reports on utilization of stents for femoral arteries have increased recently. Nitinol stents have superior patency for use in femoral arteries due to their self-expandable geometry, capacity of radial force exertion and their ability to endow grave recovery. Superelastic Nitinol stents are used to solve problems like post implantation restenosis, twist/bending limitations, inadequate dynamic behavior and insufficient radial strength [3].

Previous studies have shown that A_f temperature has a significant influence on the mechanical and clinical performance of the Nitinol self-expanding stents [4–11]. Duerig et al. [4] have shown that stent design has a vital influence on clinical performance. Kleinstreuer et al. [5] have mathematically analyzed the superelastic behavior of different NiTi-graft stents designed for supporting Abdominal Aortic Aneurysm (AAA). Koop et al. [6] have described how Nitinol properties affect the thermomechanical behavior of stents. Pelton et al. [7] have demonstrated how superelastic Nitinol can be used for making stents. Liu et al. [8] have assessed the effect of ageing on shape-setting and the superelasticity of Ti–50.7% Ni. They have shown that 500 °C and 60 min are the optimal ageing temperature and time for achieving excellent non-linear superelasticity and maximum recoverability at body temperature. Henderson et al. [9] have experimentally obtained the accurate material characteristics of Nitinol wires for use in finite element modeling. Liu and Galvin [10] have calculated critical temperatures for the pseudoelastic behavior of Nitinol. Pelton et al. [11] have presented an optimization method for the material properties of Nitinol wires usable for medical applications.

For superelastic behavior, A_f temperature should be below body temperature [4,6]. The amount of A_f depends on the restenosis volume of the artery and required stiffness [4,6].

* Corresponding author. Tel.: +98 2166165215; fax: +98 2166005717.
E-mail address: sadrnezh@sharif.edu (S.K. Sadrnezhaad).

Peer review under responsibility of Sharif University of Technology.

Production and hosting by Elsevier

1026-3098
doi:10.1016/j.scient.2012.10.024

Very low A_f results in high stiffness and increased radial resistive force, which may cause wall injury to the artery [4–8]. It has also a short fatigue-life, which makes it unsuitable for long term dynamic applications [4].

Different geometries like the coil, helical spring, woven (braided and knitted), ring (individual and sequential), cells (closed and open) in wire form and laser cut form have previously been used for stents [12,13]. Open-cell *Z*-shaped rings have separate structural elements contributing to the longitudinal flexibility of stents. Periodically connected peak-to-peak designs are commonly used in self-expanding stents, such as smart versions [12–14].

The behavior of Nitinol wire stents have been analyzed by a few authors [15–21]. Silber et al. [15] have shown the effect of stent geometric characteristics on the mechanical properties of NiTi wire stents. Beule et al. [16] have optimized the mechanics of braided stents. Petrini et al. [17] have developed a numerical model for explanation of the crushing test results. Whitcher [18] has numerically studied the fatigue behavior of NiTi for use in manufacturing stents. Numerical investigation of *Z*-shaped open-cell femoral artery self-expanding stents made of Nitinol wire seems, however, missing in the literature.

No report is, however, available on open-cell *Z*-shaped rings of Nitinol wire stents designed for femoral artery implantation. The main purpose of this study is to evaluate the effect of variations in material properties, such as A_f temperature, on the mechanical and clinical performance of the newly designed Nitinol stents for the femoral artery, using the Finite Element Method (FEM).

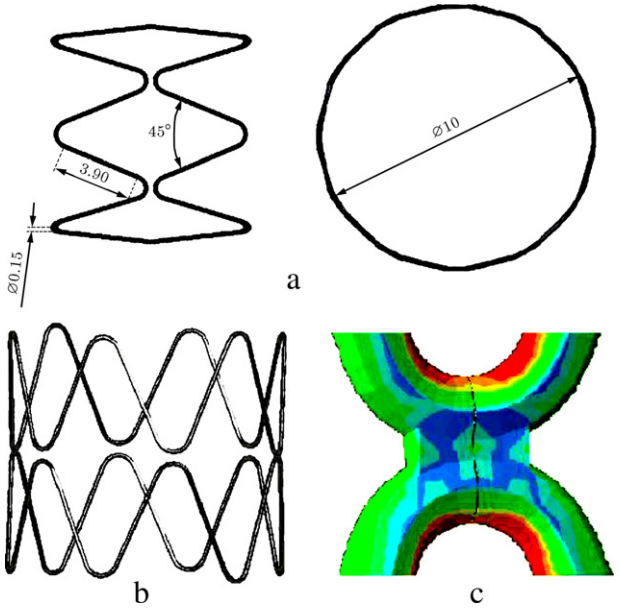

Figure 1: Geometry of two-junction stent designed in this research. Different views are shown for better understanding of the shape: (a) geometric details, (b) full stent, and (c) exact position of the junction area of the stent where numerical calculations (the amount of maximum in curves of junction area) have been performed. Stent geometry at the junction as integrated is considered. Unit of length is mm.

2. Material and methods

2.1. Geometric models

Geometries of commercially made stents are based on the strictest patents. Little information has, therefore, been given by manufacturers about the effect of geometry on the behavior of the stents. To obtain the optimum geometry, Micro-CT should, therefore, be used. The benefit of using this technique is the possibility of the direct building of a 3-D stent model.

There are not enough information and clinical reports available in the literature describing NiTi femoral stent behavior. This paper is to introduce a newly developed design of a SFA open-cell *Z*-shape wire stent usable for the treatment of femoral occlusive disease. Two sets of material properties obtained from previous research models [5,11,22,23] are used to determine the performance of the newly devised geometry. Based on the information available in the literature [1,2], Nitinol stents with new geometry, as shown in Figure 1, were designed for the femoral artery using a computer aided three-dimensional interactive application Catia v. 5 (Dassault Systèmes, USA).

2.2. Material properties

The present study is merely focused on the effect of the properties of superelastic Nitinol on the behavior of the stents designed for clinical applications. The two constitutive models used in this paper are based on approaches proposed by Auricchio et al. and by Qidwai and Lagoudas, respectively [22–29]. The Abaqus Nitinol model used is based on the work of Auricchio, Taylor and Lubliner, with extensive extensions of Rebelo [22,24–29]. Nitinol superelasticity is modeled as a predefined user material in the Abaqus 6.10 (Dassault Systèmes, Providence, RI, USA). Parameters required in the Abaqus user material subroutine for Nitinol material are summarized in Table 1. Qidwai and Lagoudas have developed constitutive models for superelastic shape memory materials based on the second law of thermodynamics (Gibbs free energy calculation). EchoBio developed a user-defined material subroutine (Umat) based on the Qidwai and Lagoudas theory [23]. Properties of materials used in the simulation are based on the Qidwai and Lagoudas model (Table 2). According to Figure 2 and Tables 1 and 2, properties of materials according to the model of Auricchio show better agreement with experimental data than Lagoudas. Therefore, the model of Auricchio is used in this work for provision of the properties of the materials.

2.3. Meshing and boundary conditions

Because of the complex geometry and small wire section of NiTi stents, hypermesh software (Altair® HyperMesh® v. 6.0) was used for meshing of the samples. Mesh parameters of a femoral Nitinol stent undergoing a crushing test is listed in Table 3. The crushing test is used owing to the occurrence of bending, buckling and compression when the stent is placed in the femoral artery. Utilizing the Abaqus/Standard v. 6.10 (Dassault Systèmes, Providence, RI, USA) only contact between the outer stent surface and surface of the inner planes is activated. The contact algorithm applied master surface precedence to crushing at the same time as the stent is set for the slave surface. Penalty, as a general method for evaluation of contact with friction coefficients, differ in ABAQUS/STD analysis. Such contact is used to enforce impermeable boundaries; it is assumed hard and with no friction. To perform the crushing test, two rigid parallel planes apply pressure on the stent in a *y* direction. The distance between planes is equal to the external diameter of the

Table 1: Properties of materials used in simulation of femoral artery opening by Nitinol stent. The data are based on the Auricchio model [5,11,22,24].

Property	Sample 1 [11,24]	Sample 2 [5]
Austenite elasticity E_A (MPa)	45 000	40 000
Austenite Poisson's ratio (ν_A)	0.33	0.46
Martensite elasticity E_M (MPa)	38 000	18 554
Martensite Poisson's ratio (ν_M)	0.33	0.46
Transformation strain (ε^L)	0.055	0.04
Loading $(\delta\sigma/\delta T)_L$ (MPa T^{-1})	6.7	6.527
Start of transformation loading σ_L^S (MPa)	590	390
End of transformation loading σ_L^E (MPa)	640	425
Reference temperature T_0 (°C)	37	37
Unloading $(\delta\sigma/\delta T)_U$ (MPa T^{-1})	6.7	6.527
Start of transformation unloading σ_U^S (MPa)	300	140
End of transformation unloading σ_U^E (MPa)	270	135
Start of transformation stress in compression σ_{CL}^S (MPa)	–	585
Volumetric transformation strain (ε_V^L)	0.055	0.04
Strain limit $\varepsilon_{\max}$ (%)	8	12
A_f temperature (°C)	11	30

Table 2: Properties of materials used in simulation of the femoral artery opening by Nitinol stent. The data are based on Lagoudas model [11,23, 24].

Material property	Value
Austenite elastic modulus (EA) MPa	35 877
Poisson's ratio (ν)	0.33
Martensite elastic modulus (EM) MPa	24 462
Density (ρ) kg/m^3	6450
Thermal conductivity (KA) w/(m K)	18
Austenite specific heat (CA) J/(kg K)	320
Austenite thermal expansion coeff. (αA) 1/K	11×10^{-6}
Martensite thermal expansion coeff. (αM) 1/K	6.6×10^{-6}
Stress influence coefficient for austenite (ρsA) MPa/K	-0.851×10^6
Stress influence coefficient for martensite (ρsM) MPa/K	-0.452×10^6
Martensite finish temperature (M_f) K	235
Martensite start temperature (M_s) K	250
Austenite start temperature (A_s) K	251
Austenite finish temperature (A_f) K	284

Table 3: Mesh parameters of Nitinol stent for femoral artery during crushing.

Material	Element type	Number of elements	Number of nodes
Stent	C3D8I	12 624	21 720
Rigid plane	R3D4	20 000	20 402

stent which is undergoing the crushing test. Contact surfaces between rigid planes and flexible stents are frictionless. The lower rigid plane is fixed in all directions. The higher rigid plane can only move in the y direction. Four stent nodes are fixed in x and z directions but can move in a y direction. Diameter reductions of 70% and 90% are applied to the y direction of the stent. The stent is unloaded completely at the end. Boundary conditions for crushing of the femoral artery stent are shown in Figure 3. Axis symmetry helps decrease model calculations by 1/4 geometrical analysis. Temperature is set at 37 °C (body temperature).

3. Results

The Nitinol stent designed for the femoral artery is illustrated in Figure 1. This paper discusses the results of 70% crushing (Figs. 4(c) and 5(c)), which is according to available

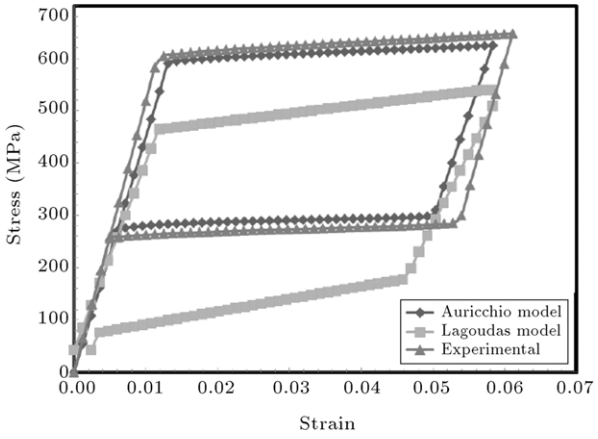

Figure 2: Comparison of Auricchio (sample 1) and Lagoudas model calculations with experimental data obtained for superelastic NiTi samples illustrated in Tables 1 and 2.

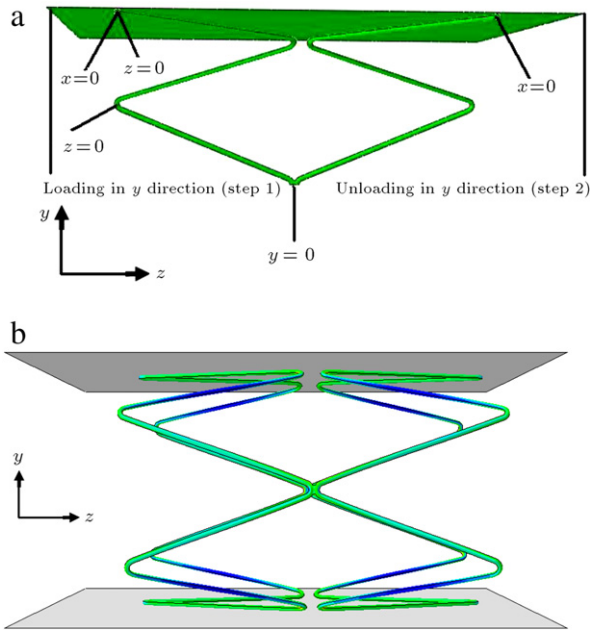

Figure 3: Schematic representation of boundary conditions for the crushing of femoral artery stent: (a) 1/4 of the stent, and (b) full stent.

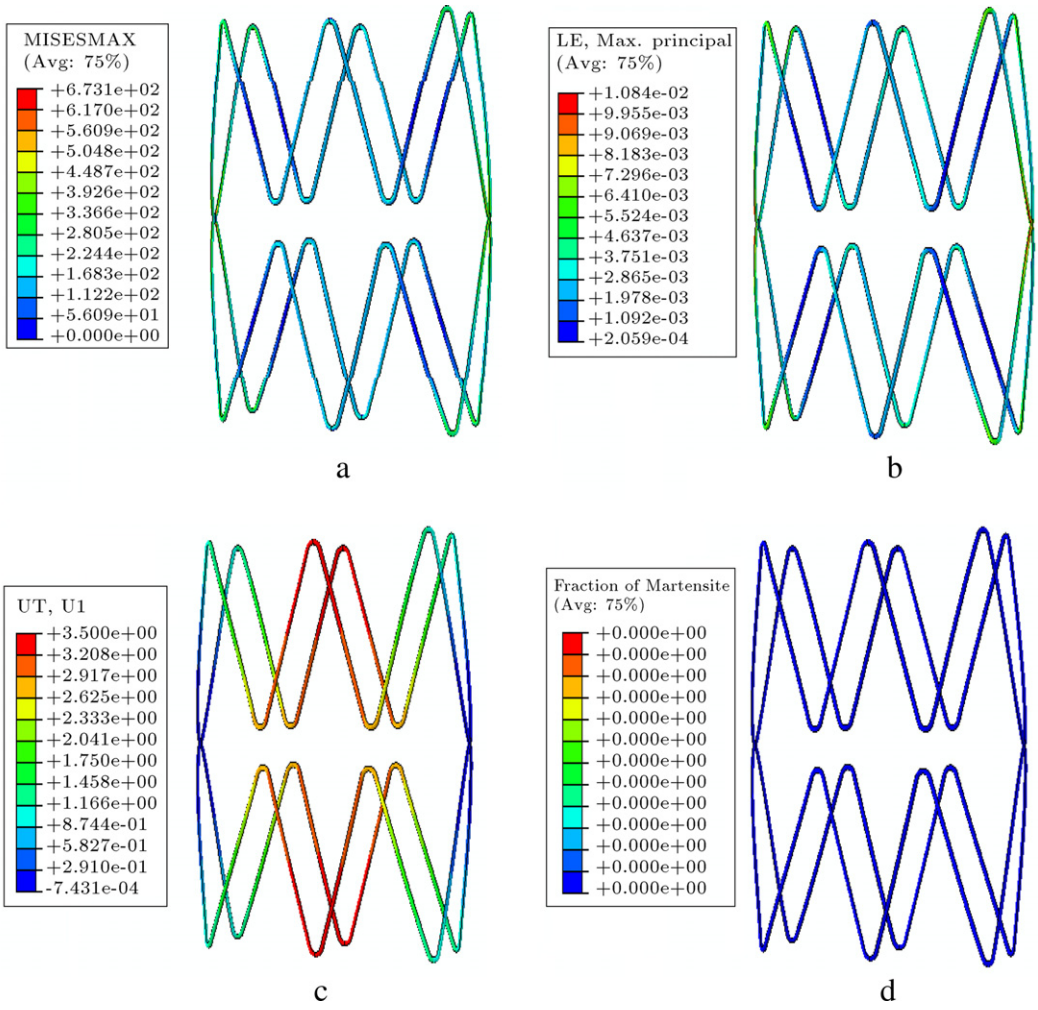

Figure 4: Result of 70% crushing of the femoral artery stents shown in Figure 1 with material properties of sample 1 of Table 1: (a) maximum Von Misses stress, (b) maximum principal strain, (c) displacement and (d) fraction of martensite formed.

Table 4: Result of stress, strain and fraction of Martensite of the femoral artery stent under 70% crushing.

Stent models	Maximum stress (MPa)	Maximum strain	Fraction of martensite
Sample 1 of Table 1	673.1	0.01084	0.0
Sample 2 of Table 1	591.2	0.01060	0.0

Table 5: Result of stress, strain and fraction of Martensite of the femoral artery stent under 90% crushing.

Stent models	Maximum stress (MPa)	Maximum strain	Fraction of martensite
Sample 1 of Table 1	731.1	0.01926	0.2958
Sample 2 of Table 1	746	0.02110	0.3295

standards [17,28,30,31]. Stresses and strains corresponding to 70% crushing of the femoral artery stents are shown in Figs. 4(a)–(b) and 5(a)–(b). Comparing Figures 4 and 5 and Table 4 indicates that a decrease in maximum stress from 673.1 to 591.2 MPa results in a decrease in maximum strain from 0.01084 to 0.01067. The fraction of martensite does not change under the same conditions. Stresses and strains corresponding to 90% crushing of femoral artery stents are shown in Figs. 6(a)–(b) and 7(a)–(b). This paper also discusses the results of 90% crushing illustrated in Figs. 6(c) and 7(c). Comparing Figures 6 and 7 and Table 5 indicates that the increase in maximum stress from 731.1 to 746 MPa results in an increase in maximum strain from 0.01926 to 0.02110. The fraction of martensite increases from 0.2958 to 0.3295 under the same conditions. By increasing the crushing level (U1) from 70% to 90%, according to Tables 4 and 5 (compare with Figures 5 and 7 for sample 2 of Table 1), the increase in maximum stress from 591.2 to 746 MPa results in an increase in maximum strain from 0.01067 to 0.02110. The fraction of martensite increases from 0.0 to 0.3295 under the same conditions. Results of numerical calculations performed for the curved junction areas of Figure 1(c), which are crushed under high pressure, are demonstrated in Figure 8.

4. Discussion

The complete mechanical hysteresis loop related to superelasticity, lowest Chronic Outward Force (COF), highest Radial Resistive Force (RRF), longest plateau stress, lower stress distribution, maximum strain distribution and the maximum percentage of martensite are useful conditions for improvement of the performance of the Nitinol stent designed for the femoral

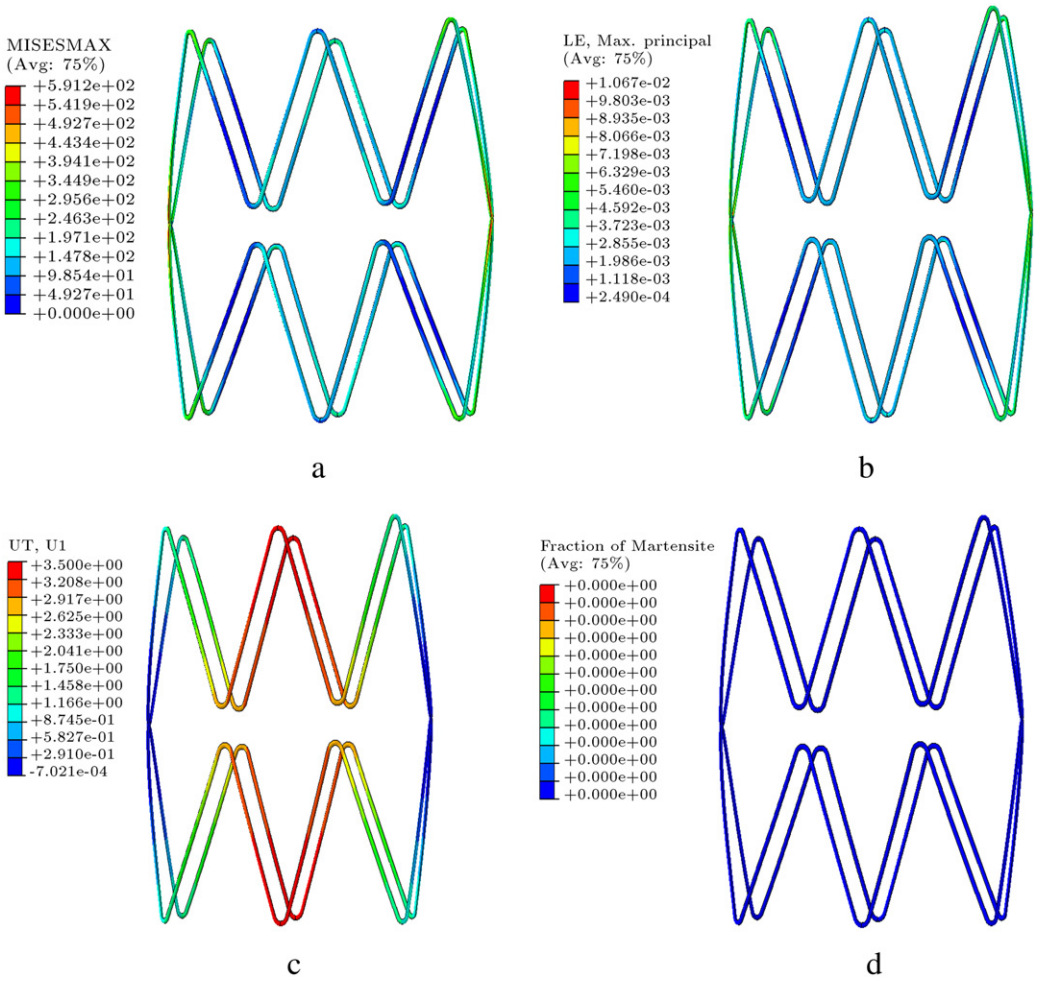

Figure 5: Result of 70% crushing of the femoral artery stents shown in Figure 1 with material properties of sample 2 of Table 1: (a) maximum Von Misses stress, (b) maximum principal strain, (c) displacement, and (d) fraction of the martensite formed.

artery [3–6,32–38]. COF and RRF are related to the superelastic behavior of the Nitinol stent. A typical superelastic stress–strain curve for the self-expanding stent is shown in Figure 9. The stent is crushed by two rigid planes (path a–b), then later deployed, reaching a stress equilibrium with the artery at point c. The force against the artery is controlled by the unloading curve (COF) and the force resisting deformation is controlled by the loading curve (RRF). Usually, stent designers attempt to get as high an RRF as possible, with as low a COF as possible [4].

Two particular points should be considered:

(1) The stents should observe the Stress Induced Martensite (SIM) region of the stress–strain curve to demonstrate suitable superelastic behavior.
(2) The stents should be used in the failure-safe domain of the stress–strain curve [31,35].

On the other hand, based on studies in this field, A_f temperature has a great effect on the good performance of the superelastic Nitinol stent [5–11,36–38]. Every Nitinol stent with high A_f temperature (close to body temperature) will be in the lower range of the COF and have a better fatigue life. Nitinol stents of acceptable performance with low restenosis of the femoral artery do not require high RRF. The A_f temperature of Nitinol should be much lower than body temperature owing to the high restenosis of the femoral artery and high RRF required for opening of the femoral artery. Previous studies have shown that lowering of A_f improves the mechanical and clinical performance of the femoral artery stents [36–38].

4.1. Evaluation of the effect of 70% crushing on the mechanical performance of femoral artery stent

According to Figures 4 and 5, Table 4 and material properties given in Table 1 for samples 1 and 2 (minimum strain to initiate martensite transformation are 0.08 and 0.12), and without the formation of martensite (Figs. 4(d) and 5(d)), the superelastic behavior of the stent is impossible. As mentioned before, the stents should observe the SIM region of the stress–strain curve to demonstrate suitable superelastic behavior [31,35]. A femoral artery stent crushed with 70% deformation did not show SIM transformation and was not suitable for the intended application.

4.2. Assessment of the effects of 90% crushing on the mechanical performance of femoral artery stent

The superelastic behavior of a stent begins with crushing of 70%–90%. It reveals that the designed stents are capable

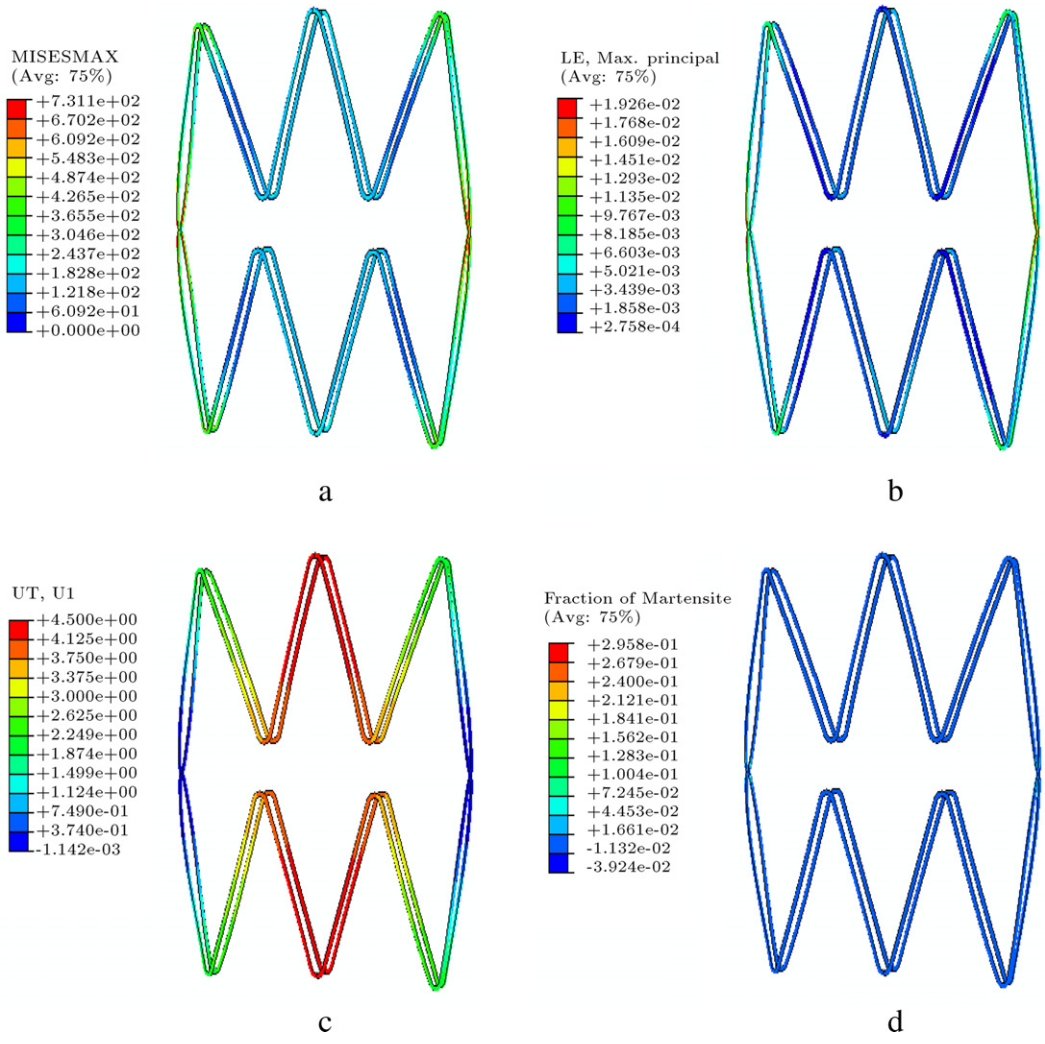

Figure 6: Result of 90% crushing of the femoral artery stents shown in Figure 1 with material properties of sample 1 of Table 1: (a) maximum Von Misses stress, (b) maximum principal strain, (c) displacement, and (d) fraction of the martensite formed.

of standing high strain forces of up to 90% and still maintain superelastic behavior. In addition, the stents are safely approached during the crushing test. According to Figures 6 and 7 and Table 5, comparing samples illustrated in Figs. 6(a) and 7(a) with maximum stress distribution on the stents internal curvature shows that there is a lower stress level on the internal curvature of the stents (sample 1 of Figure 6(a)); the former is preferred to the latter when considering the mechanical and clinical property aspects of designing these stents for application to the femoral artery. Moreover, comparing maximum strain distributions on the internal curvature of the stents in Figs. 6(b) and 7(b) indicates a higher strain level on the internal curvature of the stents (sample 2 in Figure 7(b)); the latter possesses better dynamic motion and is in greater harmony with the femoral artery circumstances. Comparing Figs. 6(d) and 7(d) about distribution of the fraction of martensite formation on the internal curvature indicates that the stents show a higher fraction of martensite formation on the internal curvature of the stents (sample 2 in Figure 7(d)).

The A_f temperature of both samples introduced in Table 1 is below 37 °C. Low A_f temperatures result in high stiffness and increased RRF, which may cause wall injury to the femoral artery [4–8]. In this case, fatigue-life would become short, which makes the stent unsuitable for long term dynamic application [4]. Every Nitinol stent with A_f close to human body temperature will be used in the lower COF and can show better fatigue life. According to Figure 8, the stent with material property 1 shows poor performance from the point of view of mechanical and clinical application, owing to very low A_f temperature, small martensite fraction, and narrow hysteresis loop related to weak superelastic behavior.

On the others hand, the lower A_f temperature of Nitinol alloys and extensive loading and unloading stress levels of mechanical hysteresis are related to the superelastic behavior. For A_f temperature difference of 7 °C, there should be approximately 50% variation in stress level [3,4]. Moreover, decreasing A_f temperature resulted in an increase in upper plateau stress [37]. Figure 8 shows an increase in upper plateau stress due to the difference between A_f temperature of 30 °C and A_f temperature of 11 °C. For A_f temperature difference of 19 °C, a variation limit of 150% is anticipated, which is confirmed by experimental and numerical results [36–38]. Consequently, based on the desired clinical and mechanical standards, the stents – according to Figure 8 – with material property 2, with less COF, higher RRF, higher fraction of martensite formation, mechanical hysteresis loop related to superelastic behavior, higher A_f temperature and more strain, show better performance from a mechanical and clinical point of view.

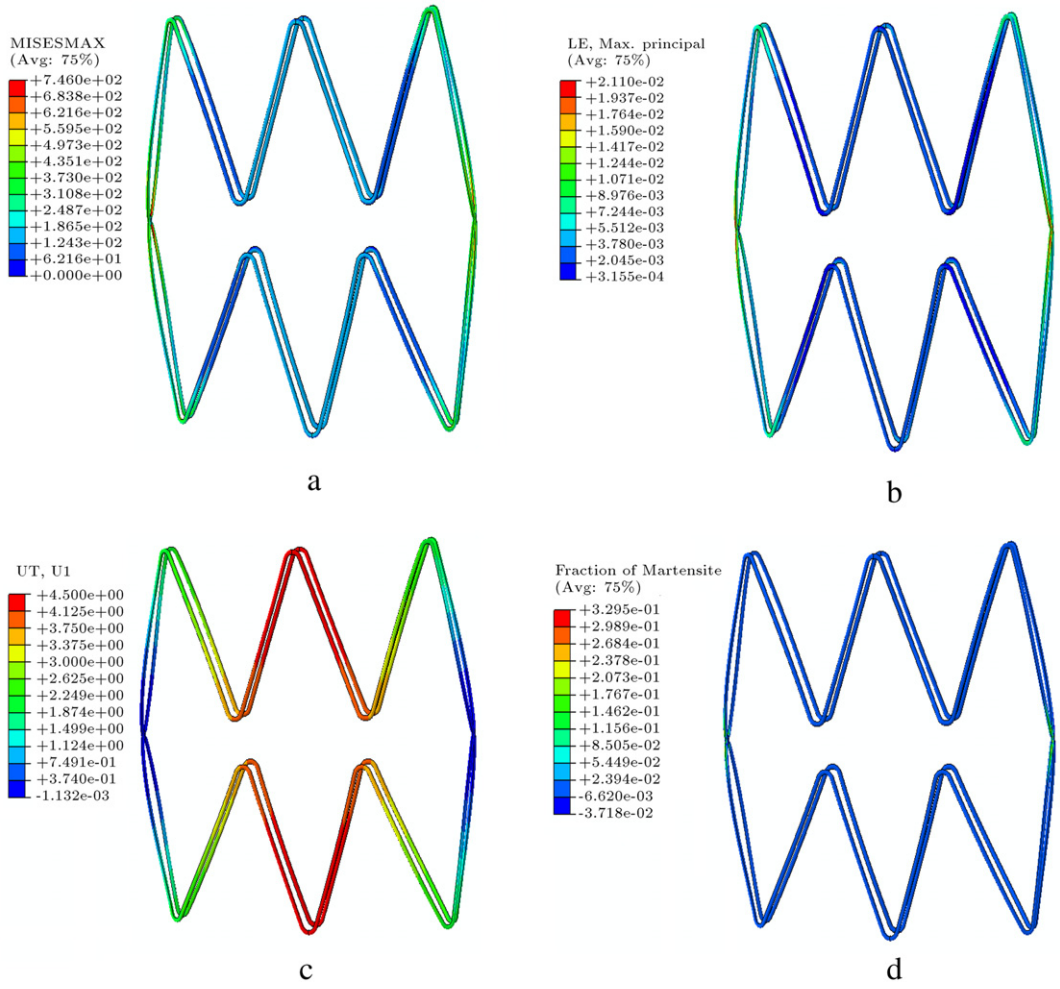

Figure 7: Result of 90% crushing of the femoral artery stents shown in Figure 1 with material properties of sample 2 of Table 1: (a) maximum Von Misses stress, (b) maximum principal strain, (c) displacement and (d) fraction of the martensite formed.

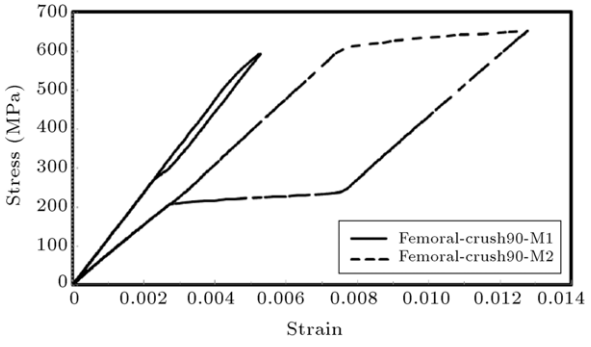

Figure 8: Comparison between superelasticity behaviors resulted from 90% crushing of the femoral artery stent shown in Figure 1(c) with material properties of samples 1 and 2 of Table 1.

4.3. Limitations

Crushing simulations are too difficult because of contact points, non-linear geometry, large deformation, sample buckling, stent bending and stress–strain non-linearity. On the other hand, according to Wu et al. [30], the self-contact phenomenon is assumed only during contact between the edges of the stent in the crushing test. Owing to the superelastic behavior of the Nitinol stent, these contacts do not cause additional stress on the edges of the Nitinol stent.

In Refs. [17,28,30,31], crushing tests have only been performed in longitudinal orientations. The reference temperature (T_0 in Table 1) has been selected by Refs. [4,6–8], as equal to 37 °C (approximate body temperature) for crushing tests. It is obvious that more experiments and simulation results related to blood pressure, friction, type and gender of plaque, stenosis degree of arteries and residual stresses are needed to reach a comprehensive conclusion.

5. Conclusions

Effects of variations in material properties on the mechanical and clinical performance of the open-cell, Z-shape femoral artery Nitinol wire stent is studied using a crushing test. Results show that Nitinol stents with higher A_f temperature have low COF, high RRF and large transformation strain. These are related to the greater martensitic phase transformation and wider mechanical hysteresis loop of the alloy. Complete superelastic behavior reveals a desirable performance from a mechanical and clinical behavior point of view.

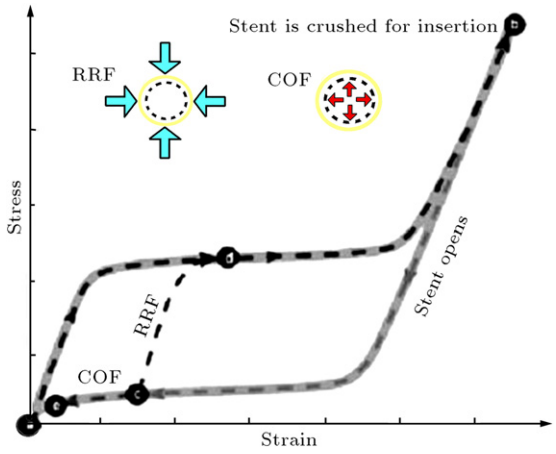

Figure 9: The RRF and COF presented as a superelastic hysteresis loop.

References

[1] Gibbs, J.M., Pena, C.S. and Benenati, J.F. "Treating the diseased superficial femoral artery", *Techniques in Vascular and Interventional Radiology*, 13, pp. 37–42 (2010).

[2] Choi, C.P.G., Herfkens, R.J. and Taylor, C.A. "The effect of ageing on deformations of the superficial femoral artery resulting from hip and knee flexion: potential clinical implications", *Journal of Vascular and Interventional Radiology*, 21, pp. 195–202 (2010).

[3] Stoeckel, D., Pelton, A.R. and Duerig, T. "Self-expanding Nitinol stents: material and design considerations", *European Radiology*, 14, pp. 292–301 (2004).

[4] Duerig, T., Tolomeo, D. and Wholey, M. "An overview of superelastic stent design", *Minimally Invasive Therapy & Allied Technologies*, 9(3/4), pp. 235–246 (2000).

[5] Kleinstreuer, C., Li, Z., Basciano, C., Seelecke, S. and Farber, M. "Computational mechanics of Nitinol stent grafts", *Journal of Biomechanics*, 41, pp. 2370–2378 (2008).

[6] Koop, K., Lootz, D., Kranz, C., Momma, C., Becher, B. and Kieckbusch, M. "Stent material Nitinol—determination of characteristics and component simulation using the finite element method", *Progress in Biomedical Research*, 6(3), pp. 237–245 (2001).

[7] Pelton, A.R., Duerig, T. and Stockel, D. "A guide to shape memory and superelasticity in Nitinol medical devices", *Minimally Invasive Therapy & Allied Technologies*, 13(4), pp. 218–221 (2004).

[8] Liu, X., Wang, Y., Yang, D. and Qi, M. "The effect of ageing treatment on shape-setting and superelasticity of a Nitinol stent", *Materials Characterization*, 59, pp. 402–406 (2008).

[9] Henderson, E., Nash, D. and Dempster, W. "On the experimental testing of fine Nitinol wires for medical devices", *Journal of the Mechanical Behavior of Biomedical Materials*, pp. 1–8 (2011).

[10] Liu, Y. and Galvin, P. "Criteria for pseudoelasticity in near-equiatomic NiTi shape memory alloys", *Acta Materialia*, 45(11), pp. 4431–4439 (1997).

[11] Pelton, A.R., DiCello, J. and Miyazaki, S. "Optimization of processing and properties of medical grade Nitinol wire", *Minimally Invasive Therapy & Allied Technologies*, 9(1), pp. 107–118 (2000).

[12] Stoeckel, D., Bonsignore, C. and Duda, S. "A survey of stent designs", *Minimally Invasive Therapy & Allied Technologies*, 11(4), pp. 137–147 (2002).

[13] Zahora, J., Bezrouk, A. and Hanus, J. "Models of stents—comparison and applications", *Physiological Research*, 56(Suppl. 1), pp. S115–S121 (2007).

[14] Patrick, B., Snowhill, B., John, L., Randall, L. and Frederick, H. "Characterization of radial forces in *Z* stents", *Investigative Radiology*, 36(9), pp. 521–530 (2001).

[15] Silber, G., Alizadeh, M. and Aghajani, A. "Finite element analysis for the design of self-expandable Nitinol stent in an artery", *International Journal of Energy and Technology*, 2(19), pp. 1–7 (2010).

[16] Beule, M., Cauter, S., Mortier, P., Loo, D., Impec, R., Verdonck, P. and Verhegghe, B. "Virtual optimization of self-expandable braided wire stents", *Medical Engineering*, 31, pp. 448–453 (2009).

[17] Petrini, L., Migliavacca, F., Massarotti, P., Schievano, S., Dubini, G. and Auricchio, F. "Computational studies of shape memory alloy behavior in biomedical applications", *Journal of Biomechanical Engineering*, 127, pp. 716–725 (2005).

[18] Whitcher, F.D. "Simulation of *in vivo* loading conditions of Nitinol vascular stent structures", *Computers & Structures*, 64(5–6), pp. 1005–1011 (1997).

[19] Migliavacca, F., Petrini, L., Massarotti, P., Schievano, S., Auricchio, F. and Dubini, G. "Stainless and shape memory alloy coronary stents, a computational study on the interaction with the vascular wall", *Biomechanics and Modeling in Mechanobiology*, 2(4), pp. 205–217 (2004).

[20] Terriault, P., Brailovski, V. and Gallo, R. "Finite element modeling of a progressively expanding shape memory stent", *Journal of Biomechanics*, 39(15), pp. 2837–2844 (2006).

[21] Auricchio, F., Conti, M., Beule, M., Santis, G. and Verhegghe, B. "Carotid artery stenting simulation: from patient-specific images to finite element analysis", *Medical Engineering and Physics*, 33, pp. 281–289 (2011).

[22] Auricchio, F. and Taylor, R. "Shape-memory alloys: modeling and numerical simulations of the finite-strain superelastic behavior", *Computer Methods in Applied Mechanics and Engineering*, 143(1–2), pp. 175–194 (1997).

[23] http://smart.tamu.edu/SMAText.

[24] Conti, M., Beule, M., Mortier, P., Loo, D., Verdonck, P., Vermassen, F., Segers, P., Auricchio, F. and Verhegghe, B. "Nitinol embolic protection filters: design investigation by finite element analysis", *Journal of Materials Engineering and Performance*, 18, pp. 787–792 (2009).

[25] Rebelo, N., Walker, N. and Foadian, H. "Simulation of implantable stents", *Abaqus User's Conference*, 143, pp. 421–434 (2001).

[26] Auricchio, F. and Taylor, R. "Shape-memory alloys: modeling and numerical simulations of the finite-strain super elastic behavior", *Computer Methods in Applied Mechanics and Engineering*, 143, pp. 175–194 (1996).

[27] Lubliner, J. and Auricchio, F. "Generalized plasticity and shape memory alloy", *International Journal of Solids and Structures*, 33, pp. 991–1003 (1996).

[28] Auricchio, F., Coda, A., Reali, A. and Urbano, M. "SMA numerical modeling versus experimental results: parameter identification and model prediction capabilities", *Journal of Materials Engineering and Performance*, 18, pp. 649–654 (2009).

[29] Arghavani, J., Auricchio, F., Naghdabadi, R. and Sohrabpour, S. "A 3-D phenomenological constitutive model for shape memory alloys under multiracial loadings", *International Journal of Plasticity*, 26, pp. 976–991 (2010).

[30] Wu, W., Qi, M., Liu, X., Yang, D. and Wang, W. "Delivery and release of Nitinol stent in carotid artery and their interactions: a finite element analysis", *Journal of Biomechanics*, 40(13), pp. 3034–3040 (2007).

[31] Auricchio, F., Conti, M., Morganti, S. and Reali, A. "Shape memory alloy: from constitutive modeling to finite element analysis of stent deployment", *Computer Modeling in Engineering & Sciences*, 57(3), pp. 225–243 (2010).

[32] Salaheldin, M., Zilla, S. and Franz, T. "A computational study of structural designs for a small-diameter composite vascular graft promoting tissue regeneration", *Cardiovascular Engineering and Technology*, 1(4), pp. 269–281 (2010).

[33] Gideon, V., Kumar, P. and Mathew, L. "Finite element analysis of the mechanical performance of aortic valve stent designs", *Trends in Biomaterials and Artificial Organs*, 23(1), pp. 16–20 (2009).

[34] Gong, X., Duerig, T., Pelton, A., Rebelo, N. and Perry, K. "Finite element analysis and experimental evaluation of superelastic Nitinol stents", *Proceedings of the International Conference on Shape Memory and Superelastic Technology Conference*—SMST (2003).

[35] Pelton, A.R., Schroeder, V., Mitchell, M., Gong, X., Barneya, M. and Robertson, S. "Fatigue and durability of Nitinol stents", *Journal of the Mechanical Behavior of Biomedical Materials*, 1, pp. 153–164 (2008).

[36] Yeung, K., Cheung, K., Lu, W. and Chung, C. "Optimization of thermal treatment parameters to alter austenitic phase transition temperature of NiTi alloy for medical implant", *Materials Science and Engineering A*, 383, pp. 213–218 (2004).

[37] Patel, M., Plumley, D. and Bouthot, R. "The effects of varying active a_f temperatures on the fatigue properties of nitinol wire", *ASM Material and Process Conference and For Medical Devices Exposition (MPMD) Boston*, MA, pp. 1–8 (2005).

[38] Otsuka, K. and Kakeshita, T. "Science and technology of shape memory alloys: new developments", *MRS Bulletin*, 27(2), pp. 91–98 (2002).

Fardin Nematzadeh was born in Ardabil, Iran, in 1976. He received his B.S. degree in Materials Science and Engineering from Sahand University of Technology, Tabriz, Iran, in 1998, and his M.S. degree in Materials Science and Engineering from Sharif University of Technology, Tehran, Iran, in 2001. He is, currently, a Ph.D. degree candidate in the Materials and Energy Research Center (MERC), Tehran, Iran. His main research interests include: modeling and simulation in medical applications such as stent, shape memory alloys, biomaterials, biomechanics and joining methods. He has published more than 25 papers in international journals and conferences.

Sayed Khatiboleslam Sadrnezhaad was born in Tehran, Iran, in 1951. He received his B.S. degree in Metallurgical Engineering from Sharif University of Technology, Tehran, Iran, in 1974, and his Ph.D. degree in Materials Science and Engineering from Massachusetts Institute of Technology, Cambridge, MA, in 1979. He is, currently, Distinguished Professor in the Department of Materials Science and Engineering at Sharif University of Technology, Tehran, Iran. He has published 3 books, 57 patents, and more than 250 papers in prestigious international journals and conferences.